

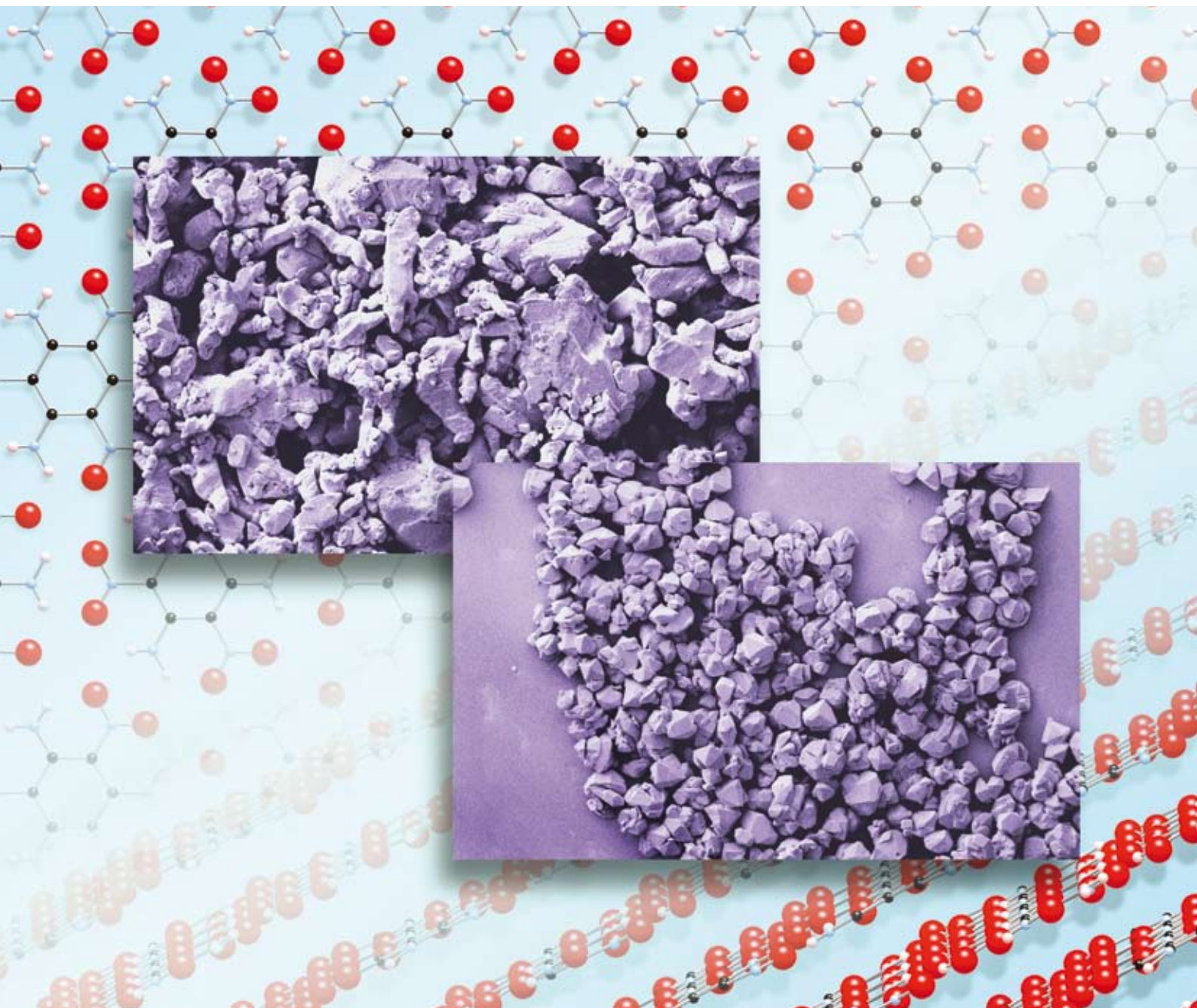
# NJC

New Journal of Chemistry

An international journal of the chemical sciences

[www.rsc.org/njc](http://www.rsc.org/njc)

Volume 33 | Number 1 | January 2009 | Pages 1–212



ISSN 1144-0546

RSC Publishing



**PAPER**

T. Yong-Jin Han *et al.*  
The solubility and recrystallization of  
1,3,5-triamino-2,4,6-trinitrobenzene  
in a 3-ethyl-1-methylimidazolium  
acetate–DMSO co-solvent system



1144-0546(2009)33:1;1-2

# The solubility and recrystallization of 1,3,5-triamino-2,4,6-trinitrobenzene in a 3-ethyl-1-methylimidazolium acetate–DMSO co-solvent system

T. Yong-Jin Han,\* Philip F. Pagoria, Alexander E. Gash, Amitesh Maiti, Christine A. Orme, Alexander R. Mitchell and Laurence E. Fried

Received (in Gainesville, FL, USA) 17th June 2008, Accepted 6th August 2008

First published as an Advance Article on the web 18th September 2008

DOI: 10.1039/b810109d

Ionic liquids have previously been shown to dissolve strong inter- and intramolecular hydrogen-bonded solids, including natural fibers. Much of this solubility is attributed to the anions in ionic liquids, which can disrupt hydrogen bonding. We have studied the solubility and recrystallization of 1,3,5-triamino-2,4,6-trinitrobenzene (TATB), a very strong inter- and intramolecular hydrogen-bonded solid, in various ionic liquid solvent systems. We discovered that acetate-based ionic liquids were the best solvents for dissolving TATB, while other anions, such as  $\text{Cl}^-$ ,  $\text{HSO}_4^-$  and  $\text{NO}_3^-$  showed moderate improvements in the solubility compared to conventional organic solvents. Ionic liquid–DMSO co-solvent systems were also investigated for dissolving and recrystallizing TATB.

## 1. Introduction

Ionic liquids (ILs) have recently been shown to be ideal solvents for dissolving hydrogen-bonded solids, including cellulose<sup>1</sup> and natural fibers.<sup>2,3</sup> The use of imidazolium-based cations with halides as counter-anions has significantly improved the solubilities of these natural products. Successful dissolution of these highly hydrogen-bonded solids is largely attributed to the ability of ILs' anions to act as hydrogen bond acceptors and disrupt the hydrogen bonds in these materials.<sup>1</sup>

With a graphite-like crystalline structure,<sup>4</sup> 1,3,5-triamino-2,4,6-trinitrobenzene (TATB) is one of the most strongly hydrogen-bonded solids known. Owing to its inter- and intramolecular hydrogen bonds, both in-plane and out-of-plane (see Fig. 1), the solubility of TATB in conventional organic solvents is minuscule. With a capacity to dissolve 70 ppm (0.007% w/v) at room temperature,<sup>5</sup> DMSO is the best conventional organic solvent known to dissolve TATB. Superacids, such as concentrated sulfuric acid, have been shown to dissolve up to ca. 240 000 ppm (24% w/v) at room temperature,<sup>5</sup> but due to their highly corrosive nature are often avoided. There is a need to find a desirable solvent for TATB as it has become necessary to control the particle size, as well as the morphology, of TATB crystals.

TATB is of particular interest in the energetic materials (EM) community due to its extreme insensitivity to impact, shock and heat, while providing a good detonation velocity.<sup>6</sup> This combination of insensitivity with good performance characteristics makes TATB an ideal insensitive high explosive (IHE) in numerous applications. TATB has also attracted researchers from the field of optics, due to its unexpectedly strong secondary harmonic generation (SHG) efficiency.<sup>7</sup> The source of the nonlinear optical (NLO) property of TATB has

been a topic of intense discussion,<sup>8,9</sup> since the original crystal structure determined by Cady and Larson showed<sup>4</sup> TATB to have a centrosymmetric structure with the space group  $\text{P}\bar{1}$ ,  $Z = 2$ , which is incompatible with NLO activity. Some have attributed the NLO activity of TATB to a small amount of a second, presently unidentified, TATB polymorph mixed in with the bulk centrosymmetric TATB crystals.<sup>10,11</sup> Therefore, identifying a suitable solvent system that can increase the

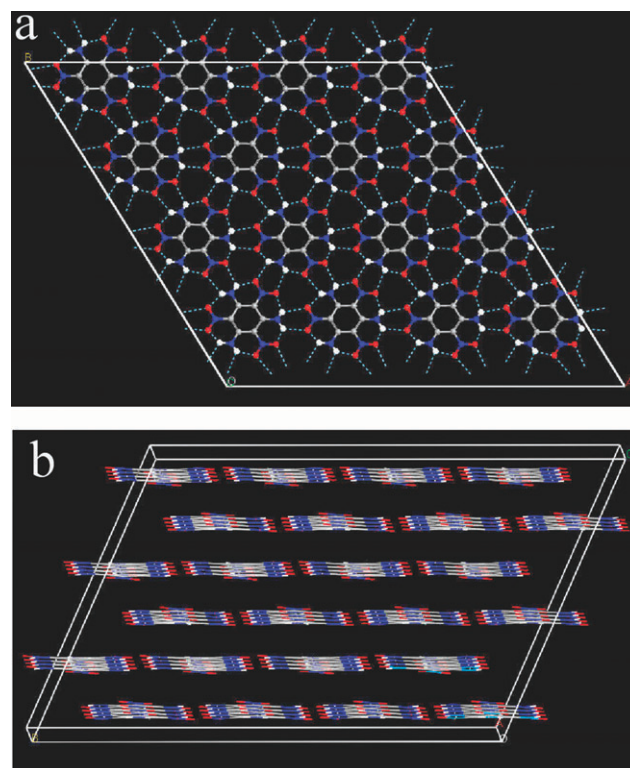


Fig. 1 The crystal structure of TATB, a centrosymmetric structure with space group  $\text{P}\bar{1}$ ,  $Z = 2$ . (a) A–B plane view, (b) C plane view.

Chemistry, Materials, Earth and Life Sciences Directorate, Lawrence Livermore National Laboratory, Livermore, CA 94551, USA.  
E-mail: han5@llnl.gov



solubility of TATB may also allow a new opportunity to crystallize and isolate the potential second polymorph with exceptional SHG efficiency.

Herein, we report the solubility of highly hydrogen-bonded TATB in both commercially available and custom synthesized imidazolium-based ILs. In particular, 3-ethyl-1-methylimidazolium acetate (EMImOAc) was extensively investigated in its pure form, as well as in combination with DMSO as a co-solvent.

## 2. Experimental

### 2.1 Materials

3-Ethyl-1-methylimidazolium chloride (EMImCl), 3-butyl-1-methylimidazolium chloride (BMImCl), 3-ethyl-1-methylimidazolium acetate (EMImOAc), 3-ethyl-1-methylimidazolium nitrate (EMImNO<sub>3</sub>), 3-butyl-1-methylimidazolium hydrogen sulfate (BMImHSO<sub>4</sub>) and DMSO were purchased from Sigma-Aldrich, and used without purification unless otherwise noted. Vacuum distillation was performed on EMImOAc to remove any impurities prior to experiments.

3-Allyl-1-methylimidazolium chloride (AllylMImCl) was synthesized according to a published report.<sup>12</sup> 3-(Methoxymethyl)-1-methylimidazolium chloride (MeOMImCl) was synthesized using a modification of the procedure reported for the synthesis of AllylMImCl.

**Synthesis of 3-(methoxymethyl)-1-methylimidazolium chloride (MeOMImCl).** Into a 500 mL round-bottomed flask equipped with a stirrer bar, argon inlet and addition funnel, was dissolved 1-methylimidazole (25 g, 0.31 mol) in trichloroethylene (100 mL). With stirring, chloromethyl methyl ether (35 g, 0.43 mol) was added dropwise over a 0.5 h period. The mixture was warmed and a turbid, two-layer mixture formed. The mixture was refluxed for 2 h, cooled and poured into a separating funnel. The organic layer was separated, filtered and the solvent removed under vacuum at 45 °C to yield a tan-beige viscous liquid (52 g).

### 2.2 Solubility measurements

Small scale solubility tests (<10 mg) of TATB in ILs were monitored with a Nikon optical microscope equipped with a temperature controlled heating stage, under cross-polarized light.

Large scale solubility measurements were performed using a three-necked round-bottomed flask in a silicone oil bath at a constant temperature of 100 °C. Due to its high density (1.93 g cm<sup>-3</sup>) and bright yellow color, visual inspection of TATB particles in solutions was easily achieved with the aid of a hand-held flashlight.

### 2.3 Crystallization

A non-agitated cooling crystallization method was employed to grow TATB crystals from a DMSO–EMImOAc co-solvent system. Typically, in a 250 mL round-bottomed flask equipped with a drying tube and a thermocouple, TATB (4 g) was added, along with 100 g of DMSO–EMImOAc (80 : 20 w/w). The solution was slowly heated to 90 °C with constant stirring. Once all of the TATB had dissolved, the solution was slowly

cooled back down to room temperature without stirring. Occasionally, an Omega (series 2010) programmable controller was used to control the cooling rate.

For a typical anti-solvent crystallization, 20 mL of an 80 : 20 DMSO–EMImOAc solution was placed in a four-necked 100 mL round-bottomed flask equipped with an overhead stirrer, drying tube, thermocouple and septum inlet. To this was added TATB (0.5 g), and the mixture was stirred and heated slightly (50 °C) until all of the TATB had dissolved and a red-orange solution had formed. The temperature of the sample was maintained at the desired temperature using a J-KEM temperature controller. The mixture was stirred slowly as a solution of acetic acid (4 g) in dry DMSO (40 mL) was added *via* a syringe and long needle connected to a syringe pump, set to deliver at 2 mL h<sup>-1</sup>. The resulting TATB was collected by suction filtration, and washed with water (25 mL) and MeOH (10 mL) to yield 0.46 g of a yellow microcrystalline solid. Raman spectroscopy was used to determine the purity of the recrystallized TATB.

## 3. Results

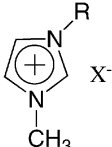
### 3.1 Solubility of TATB in ILs

There are certain advantages that ILs have over conventional solvents that make them an attractive alternative for the dissolution of TATB. ILs, because of their inherent low vapor pressure and high-temperature stability, have reduced environmental and safety concerns compared to conventional organic solvents. Also, in theory, the IL is recoverable after precipitation or distillation of impurities from it.

The solubility of TATB was first investigated in BMImCl, since BMImCl has previously been shown to dissolve cellulose,<sup>1</sup> *Bombyx mori* silk fibers<sup>2</sup> and wool keratin fibers<sup>3</sup> in relatively high concentrations (10, 13.2 and 4 wt%, respectively at 100 °C). A solution of 0.5 wt% of TATB in BMImCl was stirred rapidly at 100 °C for 20 h. However, at the end of the 20th hour, there were still TATB particles present in the flask. The color of the solution was only slightly yellow (the color of the original TATB powder), signifying that only a small amount of TATB had dissolved. Similar results were observed for other ILs with Cl<sup>-</sup> anions, including EMImCl and custom synthesized AllylMImCl (see Table 1). As noted previously, short chain-substituted imidazolium-based ILs with Cl<sup>-</sup> anions have been effective in dissolving natural polymers. The hydrogen bond-accepting Cl<sup>-</sup> anion is thought to be the crucial component in disrupting hydrogen bonding in the biopolymer.<sup>1</sup> However, for TATB the hydrogen bond disruption caused by the Cl<sup>-</sup> ions was not strong enough to significantly dissolve TATB particles.

In an attempt to improve the solubility of TATB, a new imidazolium-based cation, 3-methoxymethyl-1-methylimidazolium chloride (MeOMImCl), was synthesized. Unlike the BMIm and EMIm cations, which may have limited, if any, hydrogen bond-accepting capability, the ether side chain of MeOMImCl is a hydrogen bond acceptor<sup>13</sup> and may assist in disrupting the strong hydrogen bonding of TATB. However, when 0.5 wt% of TATB was added to MeOMImCl and heated with stirring at 100 °C for 20 h, no significant quantity of

**Table 1** The solubility of TATB in various IL systems at 100 °C

	IL	R	X <sup>-</sup>	TATB solubility (wt%)
	BMImCl	CH <sub>3</sub> CH <sub>2</sub> CH <sub>2</sub> CH <sub>2</sub>	Cl <sup>-</sup>	<0.5
	EMImCl	CH <sub>3</sub> CH <sub>2</sub>	Cl <sup>-</sup>	<0.5
	AllylImCl	CH <sub>2</sub> =CH	Cl <sup>-</sup>	<0.5
	MeOMImCl	CH <sub>3</sub> OCH <sub>2</sub>	Cl <sup>-</sup>	<0.5
	BMImHSO <sub>4</sub>	CH <sub>3</sub> CH <sub>2</sub> CH <sub>2</sub> CH <sub>2</sub>	HSO <sub>4</sub> <sup>-</sup>	<0.5
	EMImNO <sub>3</sub>	CH <sub>3</sub> CH <sub>2</sub>	NO <sub>3</sub> <sup>-</sup>	<0.5
	EMImOAc	CH <sub>3</sub> CH <sub>2</sub>	CH <sub>3</sub> COO <sup>-</sup>	10

TATB dissolved, similar to BMImCl and EMImCl, which was visually evident. This result suggests that even with an active cation, the overall hydrogen bond-accepting capacity of MeOMImCl is not significant enough to disturb the hydrogen bonding network of TATB crystals.

The effects of anions other than Cl<sup>-</sup> in dissolving TATB were also examined. For this study, BMImHSO<sub>4</sub>, EMImNO<sub>3</sub>, and EMImOAc were selected and tested. These ILs were chosen for their anions' hydrogen bond-accepting capability. As anticipated, BMImHSO<sub>4</sub> and EMImNO<sub>3</sub> had very similar results compared to BMImCl, each showing less than 0.5 wt% solubility of TATB at 100 °C. However, EMImOAc showed a surprisingly good solubility of TATB. At 100 °C in a large scale test, EMImOAc was able to dissolve up to 10 ± 1.0 wt% of TATB, confirmed by visual inspection. There was, however, a noticeable difference in the color of the acetate solution when compared to the solutions from the other anions (Fig. 2A inset). When TATB was added to EMImOAc and heated, the entire mixture turned a dark blood-red color, whereas in the other ILs, no color change was observed (at times, some turned slightly yellow, the original color of the TATB crystals). The source of this color change was investigated by UV-vis spectrophotometry. As seen in Fig. 2A, TATB added to EMImOAc (diluted 100 times with DMSO) clearly shows a pronounced peak at  $\lambda_{\text{max}} = 409$  nm, whereas TATB dissolved in DMSO only shows a TATB absorbance at  $\lambda_{\text{max}} = 357$  nm. The origin of the peak at  $\lambda_{\text{max}} = 409$  nm can be assigned to a  $\sigma$ -complex. We also carried out a Raman spectroscopy measurement of the  $\sigma$ -complex (Fig. 2B). The peaks observed at 807 and 1149 cm<sup>-1</sup> correspond well to a previously reported signature of a  $\sigma$ -complex.<sup>14</sup> The formation of a  $\sigma$ -complex with TATB was described during the synthesis of TATB by the vicarious nucleophilic substitution of hydrogen.<sup>15</sup> Selig also assigned the absorption band at 409 nm to a  $\sigma$ -complex between strong bases and TATB.<sup>5</sup>

### 3.2 Crystallization of TATB

The primary need for a solvent system that will readily dissolve TATB is to improve overall processability. More specifically, high solubility is necessary to produce high quality crystals from a supersaturated solution of TATB. Therefore, crystallization experiments were performed using EMImOAc *via* a non-agitated cooling method. An optical microscope fitted with a heating stage was used to study the recrystallization of TATB in EMImOAc. A few drops of TATB particles in EMImOAc (4 wt% solution) were placed on a cover slip on a heating stage. The mixture was heated to 100 °C and kept at

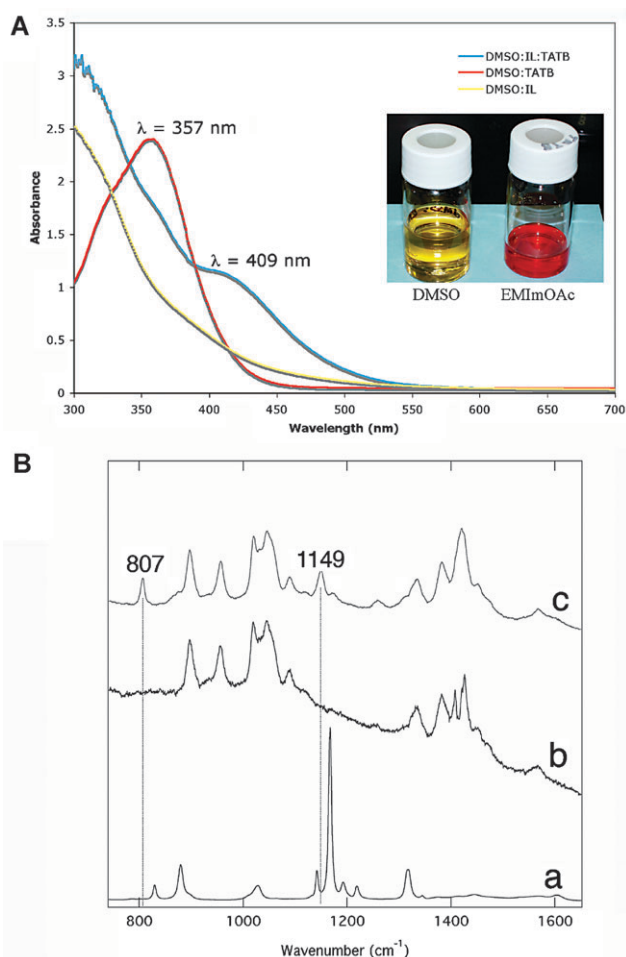


**Fig. 2** (A) UV-vis spectra of TATB dissolved in DMSO and the DMSO-EMImOAc system. The inset shows a photograph of TATB dissolved in DMSO (left) and in EMImOAc (right). (B) Raman spectra of (a) TATB, (b) EMImOAc in DMSO, (c) TATB dissolved in EMImOAc-DMSO solution; the peaks at 807 and 1149 cm<sup>-1</sup> are signatures of a  $\sigma$ -complex.

this temperature until all of the particles had dissolved (Fig. 3a and b). The homogeneous solution was cooled slowly by natural convection. From the saturated solution, crystals started to emerge when the temperature reached 70 °C. Over time, single, well-faceted crystals of TATB appeared and grew larger (Fig. 3c and d). These crystals were far better than the starting TATB crystals, which were almost all aggregates with few, if any, well defined facets.

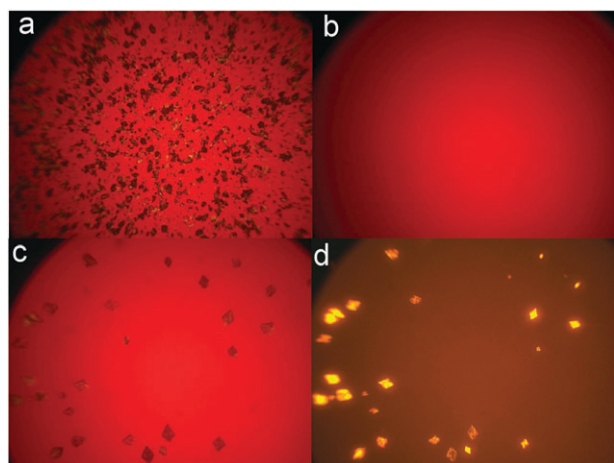


**Fig. 3** Optical images of TATB dissolving and recrystallizing in EMImOAc: (a) at room temperature, (b) at 100 °C, (c) at 70 °C and (d) cross-polarized light view of image (c).

Similar recrystallization experiments were performed on a larger scale (100 mL volume). However, due to the viscosity of EMImOAc at room temperature, it was difficult to filter and isolate the recrystallized TATB. In order to lower the viscosity of EMImOAc, DMSO was added as a co-solvent. When DMSO was added, the solubility of TATB decreased linearly with respect to the DMSO concentration (Fig. 4).

However, even with the DMSO concentration as high as 80 wt%, the solubility of TATB was still significantly high, approximately 4 wt%. Recrystallization experiments were performed using an 80 : 20 DMSO–EMImOAc solution (80 wt% DMSO, 20 wt% EMImOAc). Upon heating this solution with TATB to 90 °C, a color change was once again observed, signifying the formation of a  $\sigma$ -complex. Once the added amount of TATB had fully dissolved, the solution was allowed to cool to room temperature by natural convection, allowing crystals to form. The recrystallized TATB was recovered by simple vacuum filtration. It was visually apparent that the filtrate contained a significant amount of the  $\sigma$ -complex. Therefore, the addition of excess water or another proton donor (*i.e.* acetic acid) was necessary in order to fully recover the remaining TATB dissolved (*ca.* 1 wt%) in the filtrate. SEM

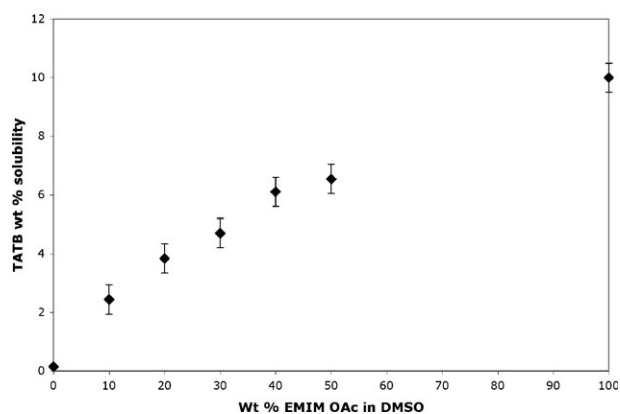


**Fig. 4** The solubility curve of TATB in the DMSO–EMImOAc system.

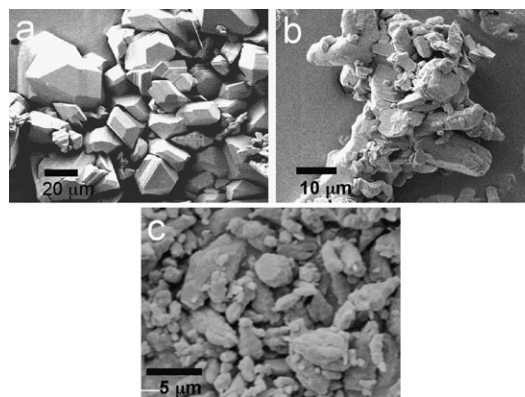


**Fig. 5** SEM micrographs of TATB (a) recrystallized from EMImOAc, (b) starting material and (c) H<sub>2</sub>O-precipitated material.

micrographs of the recrystallized TATB crystals showed good crystal morphology (Fig. 5a) compared to the starting crystals (Fig. 5b). The crystal sizes of the recrystallized TATB ranged from 10–50  $\mu$ m. On the other hand, the water crash-precipitated crystals showed an irregular crystal morphology, with crystal sizes that ranged from sub-500 nm–5  $\mu$ m (Fig. 5c). The Raman spectrum of the recrystallized TATB crystals confirmed that the structure of the recrystallized TATB matched well with that of the starting material (Fig. 6).

Besides the non-agitated cooling method of TATB crystallization, we also investigated an anti-solvent crystallization method. As seen from the non-agitated crystallization method above, a  $\sigma$ -complex, which forms when TATB is dissolved in EMImOAc, requires a proton source to fully convert it back to TATB at room temperature. Thus, we employed acetic acid as an anti-solvent to provide the necessary proton for the reaction. Acetic acid, a weak acid, was chosen to limit the rate of reaction to avoid the crash precipitation of TATB. Preliminary experiments showed that the concentration and rate of addition of acetic acid is critical in controlling the overall size of the recrystallized TATB. The overall morphology of the TATB crystals formed by this method showed a significant improvement compared to the starting materials. By carefully controlling the rate of addition, significantly large TATB crystals (<500  $\mu$ m) could be formed *via* this method.

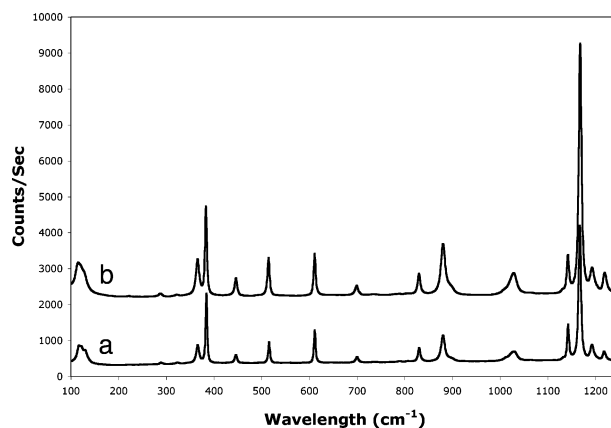


**Fig. 6** Raman spectra of (a) starting TATB and (b) recrystallized TATB.



## 4. Discussion

In order to determine the ineffectiveness of ILs in solubilizing TATB compared to cellulose, the cohesive energy density (CED) of the two systems was compared. CED is often expressed in its square-root form, known as the solubility parameter,  $\delta$ . For cellulose, a variety of measurements, including mechanical and surface free energy measurements, suggest a value of  $\delta \sim 25 \text{ MPa}^{1/2}$ .<sup>16</sup> For TATB, the heat of sublimation (*i.e.* cohesive energy per molecule) is  $\sim 40.2 \text{ kcal mol}^{-1}$ .<sup>17</sup> This, coupled with a molar volume of  $221.2 \text{ \AA}^3$  in the crystal phase,<sup>4</sup> yields a value of  $\delta \sim 35.5 \text{ MPa}^{1/2}$ . In other words, the CED ( $= \delta^2$ ) of TATB is approximately 2 times that of cellulose, explaining why the former is more difficult to dissolve than the latter. The above-obtained solubility parameter can be used as an approximate tool to screen solvents for TATB. As an example, we note that the conventional water-soluble IL,  $\text{BMIm}^+\text{BF}_4^-$ , has a solubility parameter near to  $\delta = 26.5 \text{ MPa}^{1/2}$ .<sup>18</sup> Given that TATB has a much higher value of  $\delta$ , we expect the solubility of TATB to be poor in such prototypical solvents in the absence of chemical modification. In order to understand the reason for the higher CED in TATB, we employed first-principles density functional theory (DFT) using the program DMol<sup>3</sup><sup>19–22</sup> to compute the interlayer van der Waals binding and the intralayer (intermolecular) hydrogen bond contribution to the total cohesive energy. We found that these two energies were comparable, with the van der Waals contribution being almost 90% that of the hydrogen bond contribution. The hydrogen bonds themselves have an average strength of  $\sim 3.5 \text{ kcal mol}^{-1}$ , slightly stronger than the hydrogen bonds in cellulose.<sup>23</sup>

The remarkable solubility of TATB in EMImOAc compared to other ILs was initially very puzzling. Since the cation of the ILs doesn't seem to affect the solubility of TATB, we concluded that the acetate moiety plays a key role in solubilizing TATB. TATB dissolved in EMImOAc produces a deep red color, observed at  $\lambda_{\text{max}} = 409 \text{ nm}$ . The origin of this peak can be assigned to a  $\sigma$ -complex. There are many reviews on the mechanism of the formation of  $\sigma$ -complexes in intermolecular nucleophilic displacement reactions involving electrophilic, nitro-activated aromatic substrates.<sup>24</sup> The mechanism generally involves the addition of a nucleophile to a position on the electrophilic aromatic ring that results in the stabilization of the negative charge by an *ortho*- and/or *para*-substituted nitro group. The structure of the  $\sigma$ -complex is shown in Fig. 7 and consists of a cyclohexadienyl anion, in which the carbon center that undergoes substitution is converted to an  $\text{sp}^3$ -hybridized center. The resulting negative charge may be delocalized into

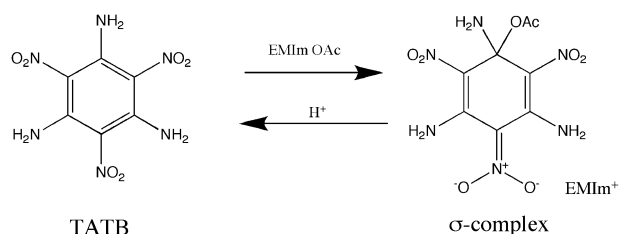


Fig. 7 Schematic of  $\sigma$ -complex formation from TATB.

the nitro groups, thus stabilizing the  $\sigma$ -complex. Most studies on the formation of  $\sigma$ -complexes investigated 1-substituted-2,4-dinitro- or 1-substituted-2,4,6-trinitrobenzenes, and very few  $\sigma$ -complexes of fully-substituted aromatic rings are known. In the TATB molecule, because of its high-symmetry, there are three equivalent positions at which the acetate anion may react to produce the  $\sigma$ -complex. The  $\sigma$ -complex would be stabilized by the presence of the three nitro groups at the 2-, 4- and 6-positions relative to the tetrahedral carbon containing the acetate group. In addition, the stability of the  $\sigma$ -complex relative to TATB would be enhanced by relieving steric crowding on the TATB ring of the adjacent amino and nitro groups upon forming the tetrahedral carbon center at the site of base addition.

TATB added to EMImCl does not form a  $\sigma$ -complex. In order to understand the difference between the action of the acetate and chloride anions on TATB, we carried out DFT-based investigations using a state-of-the-art quantum chemical conductor-like screening model (COSMO)<sup>25</sup> and its extension to real solvents (COSMO-RS).<sup>26</sup> This model computes the chemical potential of a solute in its own environment and in solvent environments. From the difference between these chemical potentials, one can estimate the solubility of the solute in the solvent. Details of the procedure are described elsewhere.<sup>27</sup> Table 2 (column 2) displays the computed solubility of TATB in EMImCl and EMImOAc, respectively. The computed solubility in EMImCl is in line with the observed low solubility (*i.e.*  $< 0.5 \text{ wt\%}$ ) in this solvent. In contrast, the computed solubility in EMImOAc is 250 times smaller than the experimentally observed value of  $10 \text{ wt\%}$  at  $100^\circ\text{C}$ . This result, in conjunction with color changes observed in the acetate IL solution, indicates that while TATB dissolves in its pure form in EMImCl, it undergoes some chemical reaction during its dissolution in EMImOAc. We have also computed the possibility of a deprotonation mechanism for the observed solubility in EMImOAc. To do this, we have investigated one of the simplest reactions, *i.e.* an  $\text{NH}_2$  group of TATB loses a proton to a neighboring anion of the IL (thereby forming an acetic acid molecule in the acetate IL or a  $\text{HCl}$  molecule in the chloride IL), while the unpaired cation of the IL binds to the *ortho* position of the deprotonated TATB anion. Column 3 of Table 2 lists the computed heat of reaction for such a chemical process using the program Dmol<sup>3</sup>.<sup>20–22</sup> The reaction is highly endothermic and clearly prohibitive in the chloride IL, but exothermic and likely to occur in the acetate IL. The above results can be qualitatively explained based on the stronger basicity of an  $\text{OAc}^-$  group compared to  $\text{Cl}^-$ . The computed UV-vis spectrum (using the semi-empirical program

Table 2 COSMO-RS results for TATB dissolution in EMImOAc and EMImCl

Solvent	TATB solubility at $100^\circ\text{C}$ (wt%) <sup>a</sup>	$\Delta E_{\text{deprotonation}}/\text{kcal mol}^{-1b}$
EMImOAc	0.04	−1.6
EMImCl	0.10	+22.0

<sup>a</sup> 1 wt% =  $1 \text{ g } 100 \text{ mL}^{-1} = 10 \text{ g L}^{-1}$ . <sup>b</sup> Energy of the reaction:  $\text{TATB} + \text{EMIm}^+\text{Anion}^- \rightarrow \text{EMIm}^+[\text{TATB}_{\text{deprotonated}}]^- + \text{H-Anion}$ ;  $\Delta E$  is positive (negative) for an endothermic (exothermic) reaction.

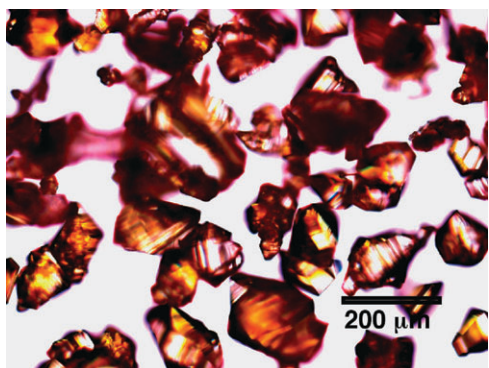


**Fig. 8** An optical micrograph of recrystallized TATB prepared by the slow cooling method.

ZINDO)<sup>28</sup> of the deprotonated TATB displayed a sharp peak at  $\sim 410\text{ cm}^{-1}$ , which is also in excellent agreement with our experimental observations. Therefore, we cannot at this point discount the possibility of alternative chemical pathways of  $\sigma$ -complex formation and the deprotonation mechanism.

We have also attempted to dissolve cellulose in EMImOAc. Although a recent report<sup>29</sup> showed a high solubility of cellulose (Avicel PH-101) in EMImOAc (15 wt%) at  $110\text{ }^{\circ}\text{C}$ , the solubility of our cellulose (Eastman Kodak) in EMImOAc at  $100\text{ }^{\circ}\text{C}$  was less than 0.5 wt%. This discrepancy can be attributed to different cellulose sources and therefore the level of recalcitrance of the cellulose tested. Our cellulose experiment result supports the idea that the mechanism of solubility for TATB in EMImOAc is indeed by chemical modification (rather than by hydrogen bond disruption). It is important to note that ILs can potentially modify the solute, as with TATB, to increase its solubility. Therefore, one must be very cautious in determining the solubility of various solutes in ILs to make sure that chemical modification of the solute is not the cause of the observed increase in solubility.

Crystallization of TATB *via* the non-agitated cooling method in EMImOAc resulted in an improved morphology of the TATB crystals obtained compared to the starting materials. Cooling by natural convection yielded crystals in the size range of  $10\text{--}50\text{ }\mu\text{m}$  (Fig. 5a). However, when the cooling rate was controlled, larger crystals were obtained. As seen in Fig. 8, when the crystallization solution was cooling at a rate of  $1\text{ }^{\circ}\text{C min}^{-1}$ ,  $200\text{--}500\text{ }\mu\text{m}$  sized crystals were obtained. One drawback of the cooling crystallization method is that at room temperature, the amount of recovered TATB is less than the original amount of TATB added, due to dissolved TATB in the 80 : 20 solution; the addition of a protic solvent is necessary to recover the remaining TATB. Thus, an anti-solvent crystallization scheme was employed as an alternative. As mentioned above, during our initial attempts to recrystallize of TATB from DMSO–EMImOAc solution, the recovery of the TATB was rather poor because it is soluble in the mixture at a 1 wt% level at room temperature. The most effective anti-solvents of all those tested were hydroxylic compounds such as organic alcohols and acids. These solvents provided a proton source that released the acetate from the  $\sigma$ -complex and precipitated the TATB. In addition, some inorganic acids, such as sodium hydrogen phosphate and boric

acid, were also found to be effective. A limiting factor in the ability of these inorganic salts to act as an efficient anti-solvent was their solubility in DMSO. Some had limited solubility, rendering them less effective in precipitating TATB in good yields. The addition of gaseous  $\text{CO}_2$  to the solvent mixture also precipitated TATB in excellent yields. It is not clear whether the  $\text{CO}_2$  acted to neutralize the mixture, making it less basic, or actually acted as a counter-solvent to precipitate the TATB. The use of gaseous  $\text{CO}_2$  is attractive because of its cost and availability, but it was hard to control the particle size of the recrystallized TATB when adding  $\text{CO}_2$  in gaseous form.

The anti-solvent of choice was acetic acid because it was reasoned that it could be removed from the IL to yield recovered EMImOAc without contamination from other salts. Preliminary results show that crystal size and shape are strongly dependent on the rate of addition and the concentration of the anti-solvent. Detailed information regarding the crystallization of TATB *via* the anti-solvent method will be published elsewhere.

## 5. Conclusion

ILs previously shown to dissolve highly hydrogen-bonded solids were ineffective with TATB. This may be due to the cohesive energy of TATB, which is almost 2 times that of cellulose. The remarkable solubility of TATB in EMImOAc was attributed to the formation of a  $\sigma$ -complex or to the deprotonation of TATB. Owing to the basicity and nucleophilicity of the  $\text{OAc}^-$  anion, the  $\sigma$ -complex could easily form in EMImOAc, but not in the presence other anions such as  $\text{Cl}^-$ . Therefore, the solubility of TATB in EMImOAc is proportional to the concentration of EMImOAc. The dissolved  $\sigma$ -complex can revert back to TATB, either *via* cooling or by the addition of an anti-solvent. The recrystallized TATB shows a much improved crystal morphology compared to the starting material. We are currently performing experiments to further control the crystallization of TATB by the anti-solvent crystallization method.

## Acknowledgements

This work performed under the auspices of the US Department of Energy by Lawrence Livermore National Laboratory under Contract DE-AC52-07NA27344. The project 06-SI-005 was funded by the Laboratory Directed Research and Development Program.

## References

- 1 R. P. Swatloski, S. K. Spear, J. D. Holbrey and R. D. Rogers, *J. Am. Chem. Soc.*, 2002, **124**, 4974.
- 2 D. M. Phillips, L. F. Drummy, D. G. Conrady, D. M. Fox, R. R. Naik, M. O. Stone, P. C. Trulove, H. C. De Long and R. A. Mantz, *J. Am. Chem. Soc.*, 2004, **126**, 14350.
- 3 H. B. Xie, S. H. Li and S. B. Zhang, *Green Chem.*, 2005, **7**, 606.
- 4 H. H. Cady and A. C. Larson, *Acta Crystallogr.*, 1965, **18**, 485.
- 5 W. Selig, Lawrence Livermore National Laboratory Report UCID-17412, 1977.
- 6 C. M. Tarver, J. W. Kury and R. D. Breithaupt, *J. Appl. Phys.*, 1997, **82**, 3771.

- 7 S. F. Son, B. W. Asay, B. F. Henson, R. K. Sander, A. N. Ali, P. M. Zielinski, D. S. Phillips, R. B. Schwarz and C. B. Skidmore, *J. Phys. Chem. B*, 1999, **103**, 5434.
- 8 J. L. Bredas, F. Meyers, B. M. Pierce and J. Zyss, *J. Am. Chem. Soc.*, 1992, **114**, 4928.
- 9 G. Filippini and A. Gavezzotti, *Chem. Phys. Lett.*, 1994, **231**, 86.
- 10 I. G. Voigt-Martin, G. Li, A. Yakimanski, G. Schulz and J. J. Wolff, *J. Am. Chem. Soc.*, 1996, **118**, 12830.
- 11 I. G. Voigt-Martin, G. Li, A. A. Yakimanski, J. J. Wolff and H. Gross, *J. Phys. Chem. A*, 1997, **101**, 7265.
- 12 H. Zhang, J. Wu, J. Zhang and J. S. He, *Macromolecules*, 2005, **38**, 8272.
- 13 M. Palusiak and S. J. Grabowski, *J. Mol. Struct.*, 2002, **642**, 97.
- 14 P. S. Santos and N. S. Goncalves, *J. Raman Spectrosc.*, 1989, **20**, 551.
- 15 A. R. Mitchell, M. D. Coburn, R. D. Schmidt, P. F. Pagoria and G. S. Lee, *Thermochim. Acta*, 2002, **384**, 205.
- 16 R. J. Roberts and R. C. Rowe, *Int. J. Pharm.*, 1993, **99**, 157.
- 17 J. M. Rosen and C. Dickinson, *J. Chem. Eng. Data*, 1969, **14**, 120.
- 18 H. Jin, B. O'Hare, J. Dong, S. Arzhantsev, G. A. Baker, J. F. Wishart, A. J. Benesi and M. Maroncelli, *J. Phys. Chem. B*, 2008, **112**, 81.
- 19 We performed all-electron calculations employing the double numeric polarized (DNP) basis set on a fine integration grid and the gradient-corrected PBE exchange correlation function. The total cohesive energy was computed by taking the difference of the total energy of a TATB unit cell (normalized per TATB molecule) from that of an isolated TATB molecule. Next, a vacuum slab normal to the basal plane was created in order to isolate the hydrogen-bonded layers of TATB from each other. The total energy of such a cell yielded a contribution to the total CED coming from just the intralayer hydrogen bond interactions.
- 20 B. Delley, *J. Chem. Phys.*, 1990, **92**, 508.
- 21 B. Delley, *J. Chem. Phys.*, 2000, **113**, 7756.
- 22 B. Delley, *Phys. Rev. B: Condens. Matter Mater. Phys.*, 2002, **66**, 155125.
- 23 B. E. Dale and G. T. Tsao, *J. Appl. Polym. Sci.*, 1982, **27**, 1233.
- 24 G. A. Artamkina, M. P. Egorov and I. P. Beletskaya, *Chem. Rev.*, 1982, **82**, 427.
- 25 A. Klamt and G. Schuurmann, *J. Chem. Soc., Perkin Trans. 2*, 1993, 799.
- 26 A. Klamt, *COSMO-RS: From Quantum Chemistry to Fluid Phase Thermodynamics and Drug Design*, Elsevier, Amsterdam, 2005.
- 27 A. Maiti, P. F. Pagoria, A. E. Gash, T. Y. J. Han, C. A. Orme, R. H. Gee and L. E. Fried, *Phys. Chem. Chem. Phys.*, 2008, **10**, 5050.
- 28 M. Zerner, *Reviews in Computational Chemistry*, VCH, New York, vol. **2**, 1991.
- 29 H. Zhao, G. A. Baker, Z. Y. Song, O. Olubajo, T. Crittle and D. Peters, *Green Chem.*, 2008, **10**, 696.